ELSEVIER

Biophysical Chemistry 62 (1996) 47–61

Biophysical Chemistry

Influence of DNA superstructural features and histones aminoterminal domains on mononucleosome and dinucleosome positioning

P. De Santis [c], B. Kropp [a], L. Leoni [b], B. Sampaolese [b], M. Savino [a,*]

[a] *Istituto Pasteur-Fondazione Cenci-Bolognetti Dipartimento di Genetica e Biologia Molecolare, Piazzale Aldo Moro, Rome 5-00185, Italy*
[b] *Centro di Studio per gli Acidi Nucleici del CNR, Piazzale Aldo Moro, Rome 5-00185, Italy*
[c] *Dipartimento di Chimica Università di Roma I 'La Sapienza', Piazzale Aldo Moro, Rome 5-00185, Italy*

Received 22 January 1996; accepted 28 May 1996

Abstract

Mononucleosome and dinucleosome positioning was studied in the complexes between two DNA fragments of different lengths, both containing a strongly curved sequence from *Crithidia fasciculata* kinetoplast, and histone octamers either normal or lacking aminoterminal domains. The results obtained by Exo III and DNase I selective digestion were:

(a) The first and most stable nucleosome, formed with both types of histone octamers, is positioned on the curved sequence, showing a multiple dyad axis translational positioning with the same rotational phasing. This result is in very good agreement with the theoretical prediction, obtained by adopting a method developed by us, based on the evaluation of DNA distortion energy from the nucleotide sequence.

(b) The second nucleosome has two main different positions. The first one, near the extremity of the DNA fragment opposite to the curved sequence, presents a higher frequency in the case of normal nucleosome, whereas an intermediate position appears populated with a higher frequency in the case of the 'tailless' nucleosome.

Keywords: DNA superstructure; Histone aminoterminal domains; Nucleosome positioning

1. Introduction

Recently, non-random nucleosome positioning on specific DNA sequences has been shown in many different biological systems as well as in synthetic DNAs [1,2]. In most cases, the main determinant of nucleosomes specific rotational positioning is associated with DNA curvature or flexibility [3,4]. This finding is not surprising, considering that nucleosomal DNA is highly bent [5].

The role of DNA superstructural features in positioning seems well established, since it is possible to predict, in fairly good agreement with experimental results in a number of cases, nucleosome positioning from the nucleotide sequence, adopting a theoretical method to localize the minima of the distortion energy required for the formation of a nucleosome-like structure by recurrent 145 bp DNA tracts [6,7]. On the contrary, the role of the histone octamer has

* Corresponding author. (Fax +39-6-4440812).

PII S0301-4622(96)02194-1

been so far an highly elusive research topic. Many research efforts have been aimed at establishing the role of the N-terminal tails of the histone core, since these regions contain a high concentration of positively charged residues and are the major sites of histone modification by acetylation and phosphorylation [8,9]. However, the results obtained, after a careful analysis by Ausio et al. [10], show that the nucleosome core stability to dissociation (below a salt concentration of 0.7 M NaCl) is not affected by the presence or absence of any of the histones N-terminal regions. Further, these histone regions contribute very little to the conformational transitions that nucleosomes undergo in this range of salt concentration. Recently, results obtained by Dong et al. [11] and by Hayes et al. [12] have shown that 'tailless' octamers and the $(H3/H4)_2$ tetramer recognise the same nucleosome positioning signals as the

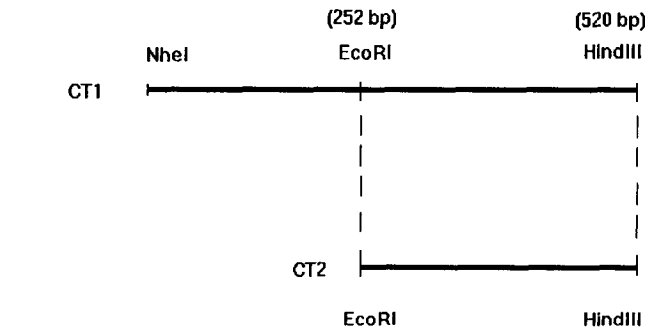

*Nhe*I
⇓
5' CTAGCGATGA CCCTGCTGAT TGGTTCGCTG ACCATTTCCG GGGTGCGGAA 50

CGGCGTTACC AGAAACTCAG AAGGTTCGTC CAACCAAACC GACTCTGACG 100

GCAGTTTACG AGAGAGATGA TAGGGTCTGC TTCAGTAAGC CAGATGCTAC 150

ACAATTAGGC TTGTACATAT TGTCGTTAGA ACGCGGCTAC AATTAATACA 200

TAACCTTATG TATCATACAC ATACGATTTA GGTGACACTA TAGAATACAC 250

*Eco*RI *Bam*HI
⇓ ⇓
GGAATTCGAG CTCGCCCGGG GATCCCG*CCT AAAATTCCAA CCGAAAATCG* 300

CGAGGTTACT TTTTTGGAGC CCGAAAACCA CCCAAAATCA AGGAAAAATG 350

GCCAAAAAAT GCCAAAAAAT AGCGAAAATA CCCCGAAAAT TGGCAAAAAT 400

TAACAAAAAA TAGCGAATTT CCCTGAATTT TAGGCGAAAA AACCCCCGAA 450

*Bam*HI
⇓
*AATGGCCAAA AACGCACTGA AAATCAAAAT CTGAACGT*CT CGGGATCCTC 500

TAGAGTCGAC CTGCAGCCCA 3'
⇑
*Hin*dIII

Fig. 1. Sequence of the *Nhe* I-*Hin*d III 520 bp DNA fragment (CT1) and of the *Eco* RI-*Hin*d III 268 bp DNA fragment (CT2). The *Bam* HI cleavage sites indicate the bent DNA sequence (211 bp) cloned in pPK201/CAT. The *Crithidia f.* curved DNA tract has been underlined.

intact octamer. In a previous work, we have studied, by topological analysis, the influence of histone tails in nucleosome assembly on minichromosomes reconstituted with trypsinized histone octamer. The topoisomers distribution, after the removal of histone tails, dramatically changes, indicating that nucleosome-nucleosome interactions remarkably decrease [13]. These findings, as well as those from Garcia-Ramirez et al. [14], on the role of histone 'tails' in the oligonucleosomes folding, suggest that the influence of histone aminoterminal domains on nucleosomal organization will have to be studied at the supranucleosomal level and in their ability to modulate the folding of the linker DNA regions. In this article we have studied the positioning of one or two nucleosomes on two DNA fragments, of different length, both containing a strongly curved sequence from *Crithidia fasciculata* kinetoplast, in order to obtain information at the molecular level, both on the role of DNA superstructural features and of histone aminoterminal domains.

2. Materials and methods

2.1. Materials

Restriction endonucleases and Bacteriophage T4 polynucleotide kinase were from USB and SIGMA. Exonuclease III (Exo III) was from Promega, Micrococcal nuclease and DNase I from Boehringer. Radiochemicals were from Amersham. Calf thymus marker histones were from SIGMA.

2.2. DNAs

The DNA fragments used were obtained by *Nhe* I-*Hin*d III (CT1) or *Eco* RI-*Hin*d III (CT2) digestion of pPK201/CAT (3,230 bp), a plasmid kindly provided by E. Di Mauro. Plasmid pPK201/CAT contains the *Stu* I-*Acc* I 211 bp bent segment from the kinetoplast DNA of the trypanosomatidae protozoan *C. fasciculata* cloned into the *Bam* HI site of the vector pSP65 [15]. The sequences of the fragments obtained with the restriction enzymes *Nhe* I, *Eco* RI and *Hin*d III are shown in Fig. 1. 5′-terminal labelling was performed according to standard procedure. Fragments labelled at one extremity were obtained as follows: plasmid DNA was restricted with a 5′-protruding enzyme, labelled and restricted with an appropriate second enzyme. The fragments were separated by 1.5% (w/v) agarose gel electrophoresis, and the band of interest was recovered by electroelution. Nucleosomal DNA was obtained from nucleosome core particles at 2.5 M NaCl treated with Proteinase K and phenol/chloroform extracted.

2.3. Nucleosomes

Nucleosome core particles were obtained from chicken erythrocytes chromatin digested with micrococcal nuclease and purified through a 5% to 20% sucrose gradient ultracentrifugation according to Forte et al. [16]. Modified nucleosomes, namely nucleosomes lacking histone N-terminal domains, were obtained from nucleosomes by digestion with immobilised trypsin according to the method developed by Ausio et al. [10]. The polyacrylamide gel electrophoresis of trypsinized histones is shown in Fig. 2(A), in comparison with normal histones.

2.4. Reconstitution procedures

The DNA fragments were reconstituted with normal and trypsinized nucleosomes according to the salt dilution protocol described by Drew and Travers [3], starting from 0.85 M NaCl to 0.05 M NaCl. The reconstitution procedures were carried out at fixed DNA/ncps ratios (ncp = nucleosome core particle).

2.5. Glycerol gradients

Reconstituted 520 bp fragments were separated from remaining free DNA and from non-specific aggregates by ultracentrifugation through a 5% to 20% glycerol gradient in 50 mM Tris-HCl(pH 7.4), 1 mM EDTA, 1 mM dithiothreitol, 0.1 mM phenylmethylsulphonylfluoride, 0.1 mg bovine serum albumin/ml, using an SW40 ultracentrifuge rotor run at 35,000 revs min^{-1} for 20 h at 4 °C. Fractions enriched in dinucleosomes were run in 0.8% agarose gel electrophoresis, in 0.5X TBE buffer, in order to extract, by electroelution, the band relative to pure dinucleosome forms (Fig. 2(B)).

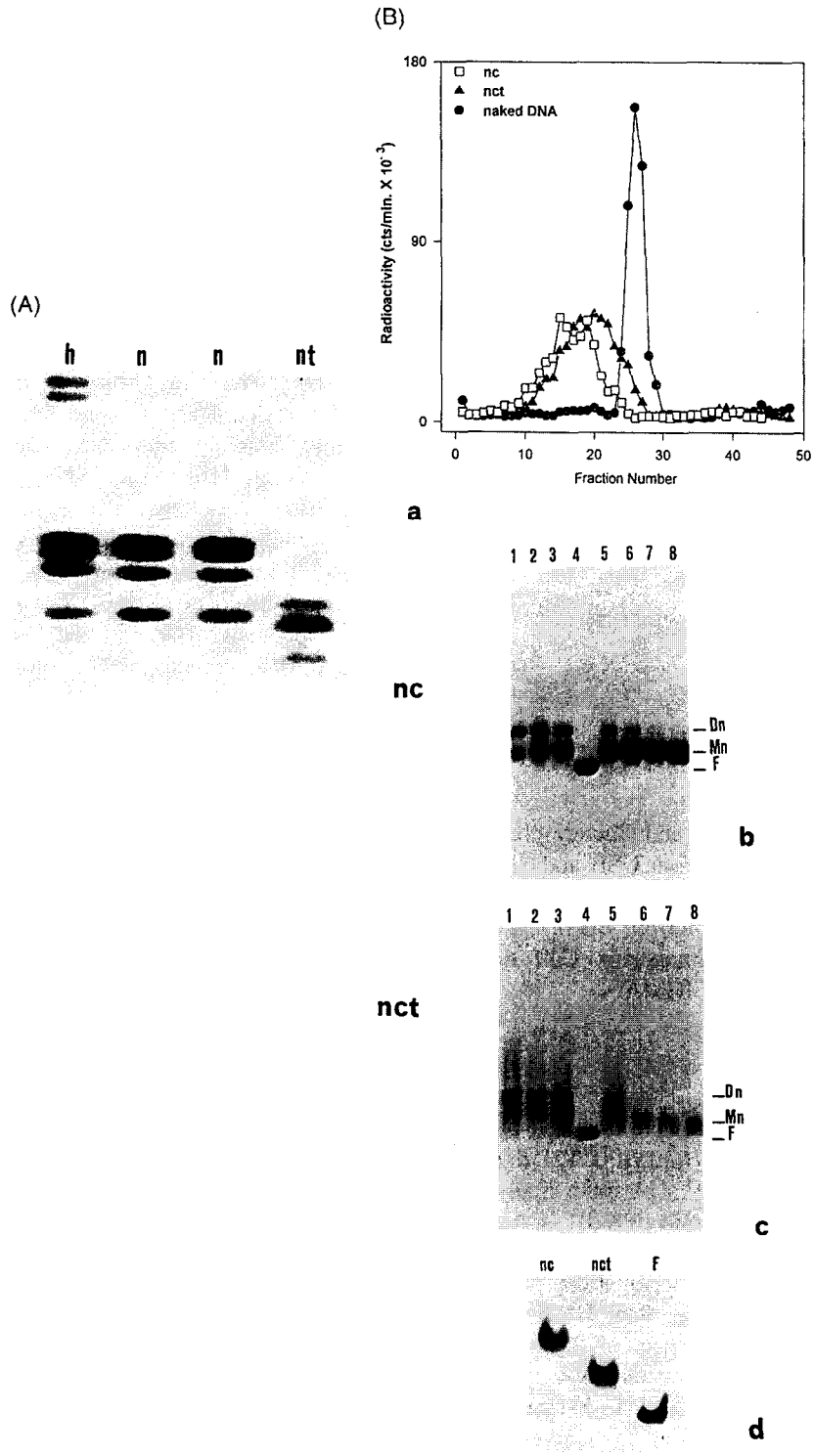
(A)
h
n
n
nt
(B)
180
90
0
nc
nct
naked DNA
Radioactivity (cts/min. X 10⁻³)
0
10
20
30
40
50
Fraction Number
a
nc
1 2 3 4 5 6 7 8
Dn
Mn
F
b
nct
1 2 3 4 5 6 7 8
Dn
Mn
F
c
nc
nct
F
d

2.6. Exonuclease III digestion

Reconstituted samples were made 66 mM Tris-HCl (pH 8), 3 mM $MgCl_2$, 1 mM 2-β-mercapto-ethanol, and incubated for 30′ at 30°C with 1200 U ml^{-1} of Exo III. The ratio between the enzyme units and the DNA amount, in all cases, was not higher than 8 U/μg. The reaction was stopped by adding an equal volume of 15 mM EDTA, 1% (w/v) sodium dodecylsulphate, and heating 2′ at 100°C [17]. The detailed experimental conditions were as reported by Buttinelli et al. [18], with only minor modifications, to eliminate the risk of strand invasion. Following extraction with phenol and precipitation with ethanol, the samples were analysed on 6% denaturing polyacrylamide gels. The gels were dried and autoradiographed; autoradiographs were analysed with a Biorad laser densitometer.

2.7. DNase I digestion

Reconstituted samples were made 11 mM $MgCl_2$ and incubated for 1′ at 37 °C with 3 U ml^{-1} of DNase I. The reaction was stopped by adding 26 mM EDTA and, after DNA extraction and precipitation, the analysis performed as described for Exo III digestion.

3. Results

3.1. Theoretical prediction of DNA superstructural features and nucleosome positioning

The superstructural features of the two fragments containing the *Crithidia fasciculata* curved sequence, *Nhe* I-*Hin*d III (520 bp) CT1 and *Eco* RI-*Hin*d III (268 bp) CT2, were derived adopting a theoretical method, previously developed by us [7], based on the integration of the slight deviations from the standard B conformation of the 16 possible dinucleotides, calculated by energy minimization. The results, reported in Fig. 3(A), show that the *C.*

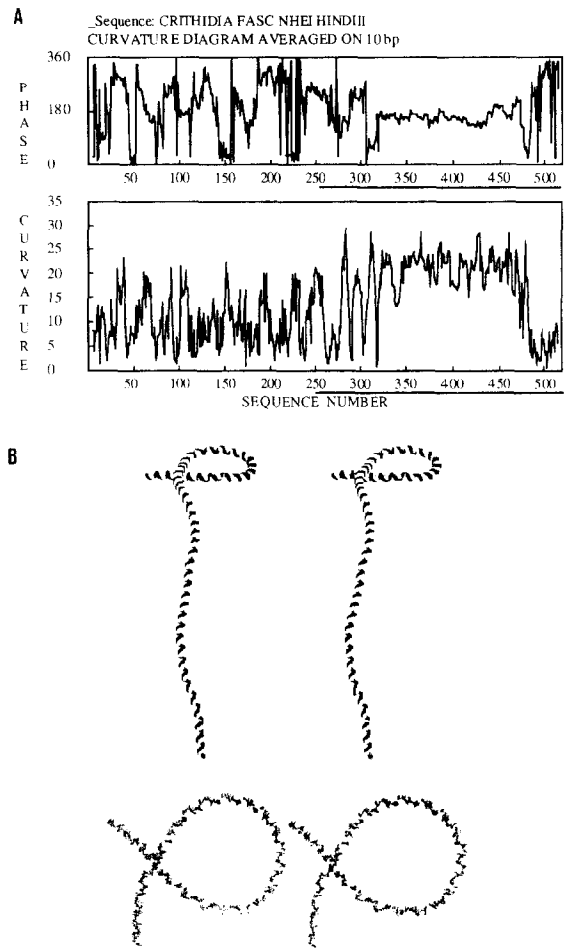

Fig. 3. (A) Curvature diagram, averaged on 10 bp, of the CT1 DNA fragment. The underlined sequence corresponds to CT2. (B) At the top, stereoview of CT1 superstructure, at the bottom, stereoview of CT2 superstructure.

Fig. 2. (A) 18% SDS-Polyacrylamide gel electrophoresis of histones. h) whole calf thymus histones as marker; n) histones derived from chicken erythrocytes nucleosomes; nt) histones derived from nucleosomes previously digested with trypsin. (B) a) Glycerol gradient analysis of reconstituted dinucleosome and mononucleosome on 5′-labelled 520 bp DNA fragments, complexed with normal (nc) and trypsinized (nct) histone octamer. Naked DNA is reported as a control. Electrophoretic analysis of some of the fractions of the gradients shown in a) is reported in b) from 12 to 24 each two fractions and c) from 14 to 26 each two fractions (from left to right). d) Dinucleosome, with normal (nc) and trypsinized histone octamer (nct), obtained by band extraction from the gel. (Dn, dinucleosome; Mn, mononucleosome; F, naked DNA).

fasciculata curved sequence, characterized by an almost constant phase in CT2 (see the underlined sequence tract), is connected to a tract of almost straight DNA in the longer fragment CT1. As it is possible to observe, in the stereoviews in Fig. 3(B), the two fragments look like: a circle (CT2) and a hook (CT1). These superstructural features result in fairly good agreement with electron microscopy visualization of CT1 and CT2 carried out by Griffith et al. [19] as we have previously shown [20]. Further, previous results [21] have shown that the *C. fasciculata* curved sequence acts as a 'nucleosome attractor', suggesting that CT1 and CT2 can be considered a useful model system to study the influence of DNA superstructural features and histone domains on the organization of mononucleosome and dinucleosome. In fact, the first and most stable nucleosome should be positioned exclusively on the *C. fasciculata* sequence and could allow to evaluate the histone aminoterminal domains influence on its positioning and stability, whereas the second nucleosome should be located along the straight part of the hook, allowing to evaluate nucleosome-nucleosome interactions either in the case of normal nucleosome or of nucleosome lacking histone aminoterminal domains. This model hypothesis was also supported by the theoretical analysis of nucleosome positioning on the two fragments.

Nucleosome positioning along a DNA sequence is defined by two parameters. The translational parameter, marking where the histone octamer dyad axis is, with respect to the direction of the average curvature, and the rotational parameter that appears to involve superstructures where the A/T rich minor grooves face in towards the protein core. Whereas the rotational parameter appears to depend exclusively on the nucleotide sequence, the signals for the translational positioning of the nucleosome dyad axis appear elusive. Recently, we have developed a theoretical method in order to obtain the virtual nucleosome positioning from the sequence by localizing the minima of the DNA distortion energy function. This was

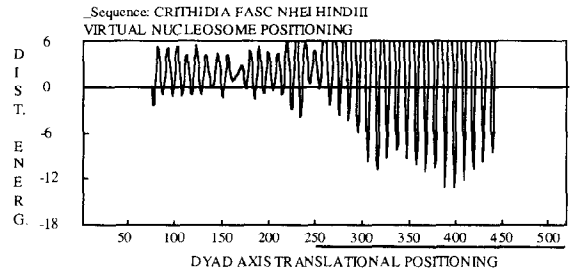

Fig. 4. The distortion energy (Kcal mole^{-1} of nucleosome) of recurrent 145 bp DNA tracts, with respect to that of an equivalent tract of straight DNA represented by the zero line, for each of the possible positions of nucleosome dyad axis, in the case of CT1 (the underlined sequence corresponds to CT2). Each minimum represents a virtual position of a nucleosome spanning a DNA tract of 73 bp on both sides. The average distance between the minima is 10.3, as evaluated via Fourier transform.

evaluated adopting our theoretical method of the sequence dependent curvature and assuming a principle of minimum deformation energy (in a simple harmonic approximation) of the intrinsic superstructure necessary to obtain the nucleosomal induced superstructure [22]. Therefore, recurrent 145 bp tracts of DNA sequence were constrained to deform in agreement with an 'open model' of the nucleosomal superstructure, characterized by two 60 bp tracts of a regular superhelix of 3/4 turns, with 43 Å radius and 28 Å pitch, interconnected by a straight tract 25 bp long. Such a model contains a dyad axis perpendicular to the superhelical axis and was adopted on account of the intrinsic superstructural features of a large collection of nucleosomal DNAs.

If c(n) and c′(n) are the starting intrinsic curvature function of a 145 bp DNA tract and the final nucleosomal curvature function, the deformation potential energy, adopting the first order elasticity model, is given by

$$E = 1/2b\langle[(c(n) - c'(n)]|[c(n) - c'(n)]\rangle$$

namely a quantity proportional to the square of the

Fig. 5. (top) Autoradiographies of Exo III digestion patterns of CT2 (5′-labelled at the *Eco* RI site on the left, and at the *Hind* III site on the right) complexed with normal (nc) or selectively trypsinized histone octamer (nct). 1) naked DNA; 2) Exo III digested naked DNA; M) *Hpa* II digest of pUC18. (bottom) Normal and trypsinized nucleosome dyad axis positioning derived from Exo III stop patterns of CT2, labelled on both sides.

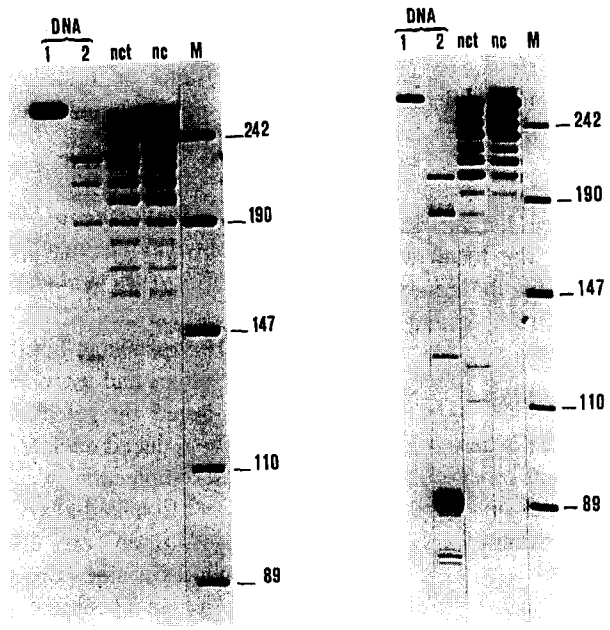
DNA
1 2 nct nc M
242
190
147
110
89
DNA
1 2 nct nc M
242
190
147
110
89

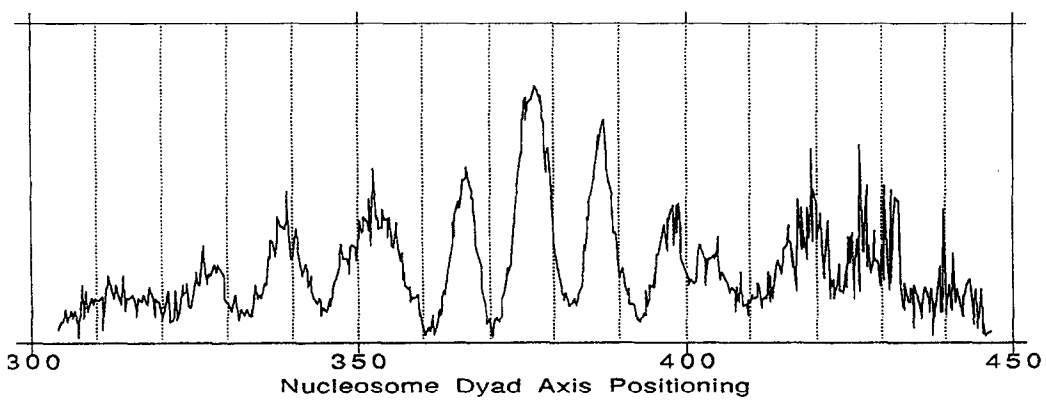
300
350
400
450
Nucleosome Dyad Axis Positioning

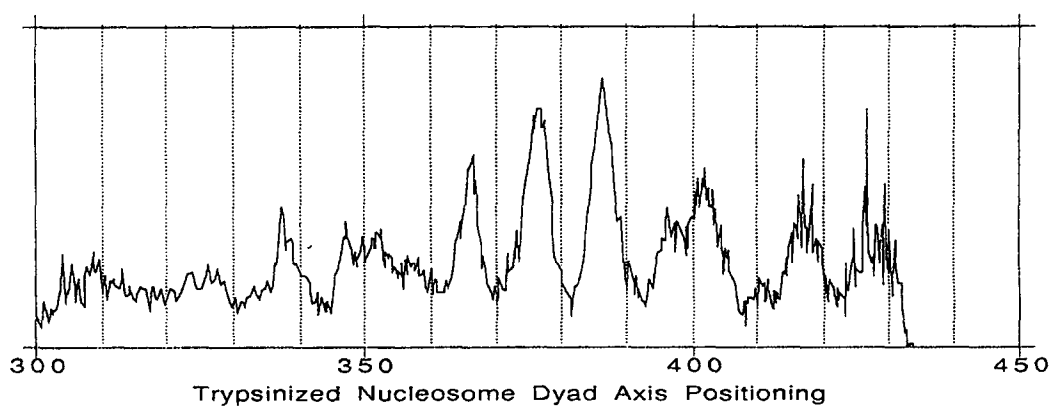
300
350
400
450
Trypsinized Nucleosome Dyad Axis Positioning

modulus of the vectorial difference between the local curvatures, averaged over a 145 bp tract, where

$$c(n) = \Sigma_{nthturn} d(s) \exp(2\pi i s/\nu)$$

is the curvature at position n of the sequence given in modulus and phase; b, the isotropic elastic bending constant of the 145 bp DNA tract

$$b = RTP/3.4 \cdot 145/\nu^2$$

$P = 450$ Å, the DNA persistence length; ν, the B DNA periodicity; $d(s) = \rho - i\tau$, the local deviation of the s_{th}. dinucleotide step from the canonical B DNA structure in terms of the roll, ρ, and tilt, τ, angles; and

$$c'(n) = -k \exp[2\pi i(n - 73)\alpha/145]$$

($k = 43.5°$ except for $60 \leq n \leq 85$ where $k = 0$); α, the pitch angle of the nucleosomal superhelix $= tg^{-1} 28/(2\pi 43))$, namely the arcotangent of the ratio between the pitch and the projection of a superhelical turn.

The energy values are given with respect to that of a straight DNA tract.

Fig. 4 shows the distortion energy profiles obtained for CT1 (the DNA tract corresponding to CT2 is underlined) by calculating, for recurrent 145 bp tracts along the sequence, the vectorial difference between the local curvature of the nucleosomal form with both phases referred to the same central 73rd bp. The periodical patterns represent the phasing between the intrinsic and induced curvatures of recurrent 145 bp tracts at the virtual positions of the dyad axis of a nucleosome.

The main features of the theoretical predicted nucleosome positioning can be summarized as follows:

(a) the first and most stable nucleosome must be positioned on the *C. fasciculata* curved sequence and is characterized by a number of dyad axis positions with the same rotational phase;

(b) the second nucleosome should occupy the first and/or the second of the two sets of shallow minima, centred at about 100 and 240 bp. These two sets are translationally degenerated, having both a number of positions with the same rotational phase. It is worth noting that the two sets are out of phase. The preference of the second nucleosome for one of the two minima could depend on interactions with the first one.

3.2. Monitoring of the exchange between nucleosomes and the two DNA fragments, containing the highly curved sequence from Crithidia fasciculata

The exchange between normal or trypsinized nucleosomes and the CT1 or CT2 DNA fragments was monitored by gel electrophoresis, taking advantage of the reduced nucleosome mobility on account of its higher molecular weight and reduced charge with respect to naked DNA. We have tried to monitor the reconstitution on 4% polyacrylamide gel electrophoresis, since this type of gel is highly selective in such band shift experiments. However, the two fragments, owing to their curvature, show an anomalously high electrophoresis mobility, with respect to their molecular weights, on polyacrylamide gels. On the contrary, in agarose gels, the two fragments show an electrophoretic mobility in agreement with their molecular weights, allowing to monitor the reconstitution reaction. In the case of the 268 bp DNA fragment, under the chosen reconstitution conditions, only one band is present, which can be easily, in all the experimental conditions adopted, attributed to a mononucleosome. The reconstituted complexes with the 520 bp DNA fragment show two bands, which can be attributed to dinucleosome and mononucleosome respectively. In order to isolate the two complexes, glycerol gradient centrifugation was used. Glycerol gradient analysis, both in the case of normal or trypsinized nucleosome, see Fig. 2 (a, b, c), indicates that, whilst it is possible to obtain pure mononucleosome, dinucleosome always appears to contain a certain amount of mononucleosome. In

Fig. 6. (top) Autoradiographies of Exo III digestion patterns of CT1 complexed with normal (nc) or selectively trypsinized histone octamer (nct). a) CT1 5′-labelled at the *Nhe* I site; b) CT1 5′-labelled at the *Hind* III site; c) amplified region of CT1 5′-labelled as in b). 1) naked DNA; 2) Exo III digested naked DNA; M) *Hpa* II digest of pUC18; M1) 123 bp DNA ladder; M2) *Hpa* II digest of pBR322. (bottom) Normal and trypsinized nucleosome dyad axis positioning derived from Exo III stop patterns of CT1, labelled on both sides.

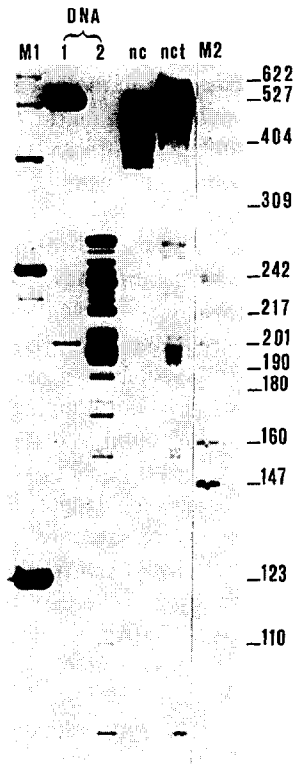
DNA
M1
1
2
nc
nct
M2
622
527
404
309
242
217
201
190
180
160
147
123
110

a

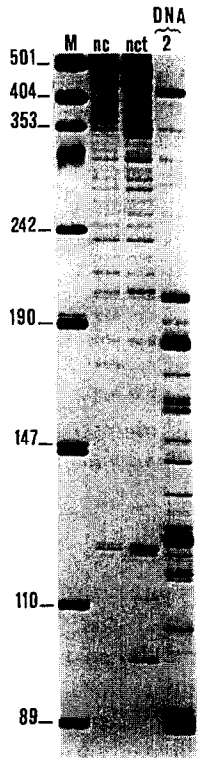
DNA
M
nc
nct
2
501
404
353
242
190
147
110
89

b

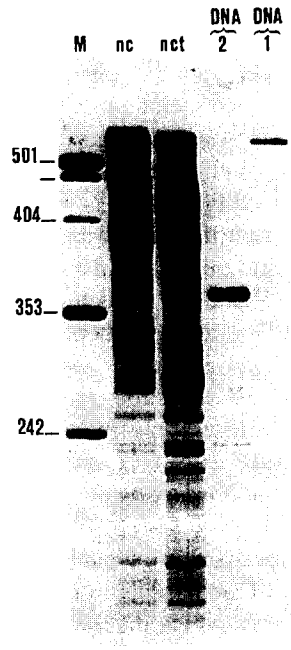
DNA
DNA
M
nc
nct
2
1
501
404
353
242

c

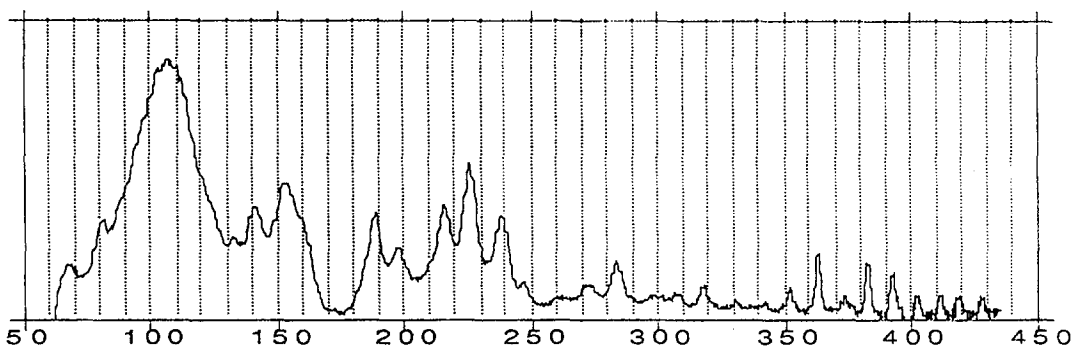
50
100
150
200
250
300
350
400
450
Nucleosome Dyad Axis Positioning

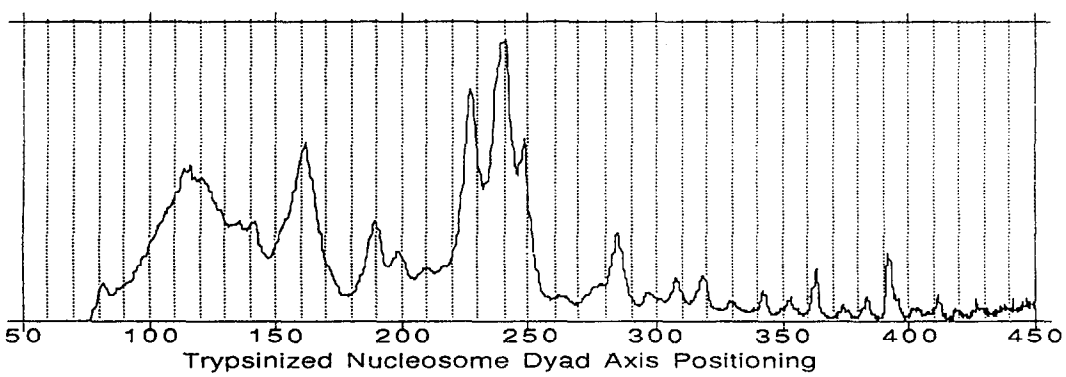
50
100
150
200
250
300
350
400
450
Trypsinized Nucleosome Dyad Axis Positioning

order to obtain pure dinucleosome, after gradient centrifugation, some fractions were separated on an agarose gel and the dinucleosome band was extracted by electroelution. A following electrophoretic analysis shows a homogeneous population of dinucleosome, both in the case of normal or trypsinized octamer (see Fig. 3d). It is worth noting that glycerol gradient centrifugation was also used for separating the reconstituted material from remaining free DNA and small amounts of non-specific aggregates, present after the reconstitution reaction.

3.3. Exo III digestion of the complexes between normal or trypsinized histone octamer and the two curved fragments CT1 and CT2 allows to obtain nucleosome borders by the enzyme stops

The localization of nucleosome borders was obtained by Exo III digestion; in fact the progress of this enzyme, which digests starting from the 3′ end, is impeded by the presence of a nucleosome. Prominent pauses, in the time course of Exo III digestion, should therefore signal the presence of major nucleosome positions. The experimental conditions were chosen so as to avoid the Exo III nucleosome invasion, as demonstrated by Buttinelli et al. [18]. We have previously shown that, under these conditions, two indipendent methods, namely Exo III digestion and micrococcal nuclease digestion with specific restriction cleavage, give rise to the same pattern of nucleosome multiple translational positioning [23].

Fig. 5 (top) shows Exo III digests of the naked DNA and the reconstituted nc or nct on the *C. fasciculata* fragment (CT2) 5′ end labelled on either strand. Since the naked *C. fasciculata* DNA shows some bands, probably as a result of sequence specific pausing of the enzyme (see Fig. 5 top, lane 2), care was taken to carry out Exo III digestions in the absence of naked DNA, as discussed in the previous section.

The band patterns of the reconstituted nc or nct, as shown in Fig. 5 (top), appear complex, indicating that the formed nucleosome, in both cases, have more than one preferential location on the considered sequence, and that a number of differently populated sets of molecules with one well positioned nucleosome are present.

To localize nucleosome stops with respect to the DNA sequence, the band patterns have been analysed as densitometric tracings. Eleven main positions, assigned considering the Exo III digestion from both directions, are detectable on reconstituted nc or nct (Fig. 5 bottom). It is worth noting that Exo III stops are considered and numbered if their distance on the two DNA strands is equal to 146 ± 4 bp, corresponding to the nucleosome length. The main result of this analysis is the equivalence of nucleosome dyad axis multiple translational positions, with constant rotational phase, both in the case of normal or selectively trypsinized nucleosome.

Exo III studies on the fragment CT1 are more complex. In this case, the DNA fragment 5′-labelled at the *Nhe* I extremity, when reconstituted as dinucleosome, after Exo III digestion, shows only few bands ranging between 520 and 470 bp, as shown in Fig. 6 (top).

The analysis of nucleosome dyad axis positions was therefore carried out assuming that the first nucleosome corresponds to that positioned on the *C. fasciculata* curved sequence as in CT2. This assumption is very reasonable, considering that it appears supported by the study of mononucleosome positioning on CT1 (data not shown). Also in this case the complex band patterns were analysed as densitometric tracings.

The main results, as shown in Fig. 6 (bottom), suggest a nucleosome multiple translational positioning, clustered in two main band families, centred at the same positions in the case of normal or selectively trypsinized nucleosome. It is worth noting

Fig. 7. (top) Autoradiographies of DNase I digestion patterns of CT2 (5′-labelled at the *Eco* RI site on the left, and at the *Hin*d III site on the right) complexed with normal (nc) or selectively trypsinized histone octamer. The two halves of each autoradiography show the products of the same digestion experiment, run on the same gel, for different times in order to extend the resolution. (1) DNase I digested naked DNA; (2) naked DNA; M) *Hpa* II digest of pUC18; G) positions of guanine in the sequence. (bottom) Densitometric tracings of nc - bold faced - and nct (a), and of nc - bold faced - and naked DNA (b) (data derived from the CT2 5′-labelled *Hin*d III site DNase I experiment).

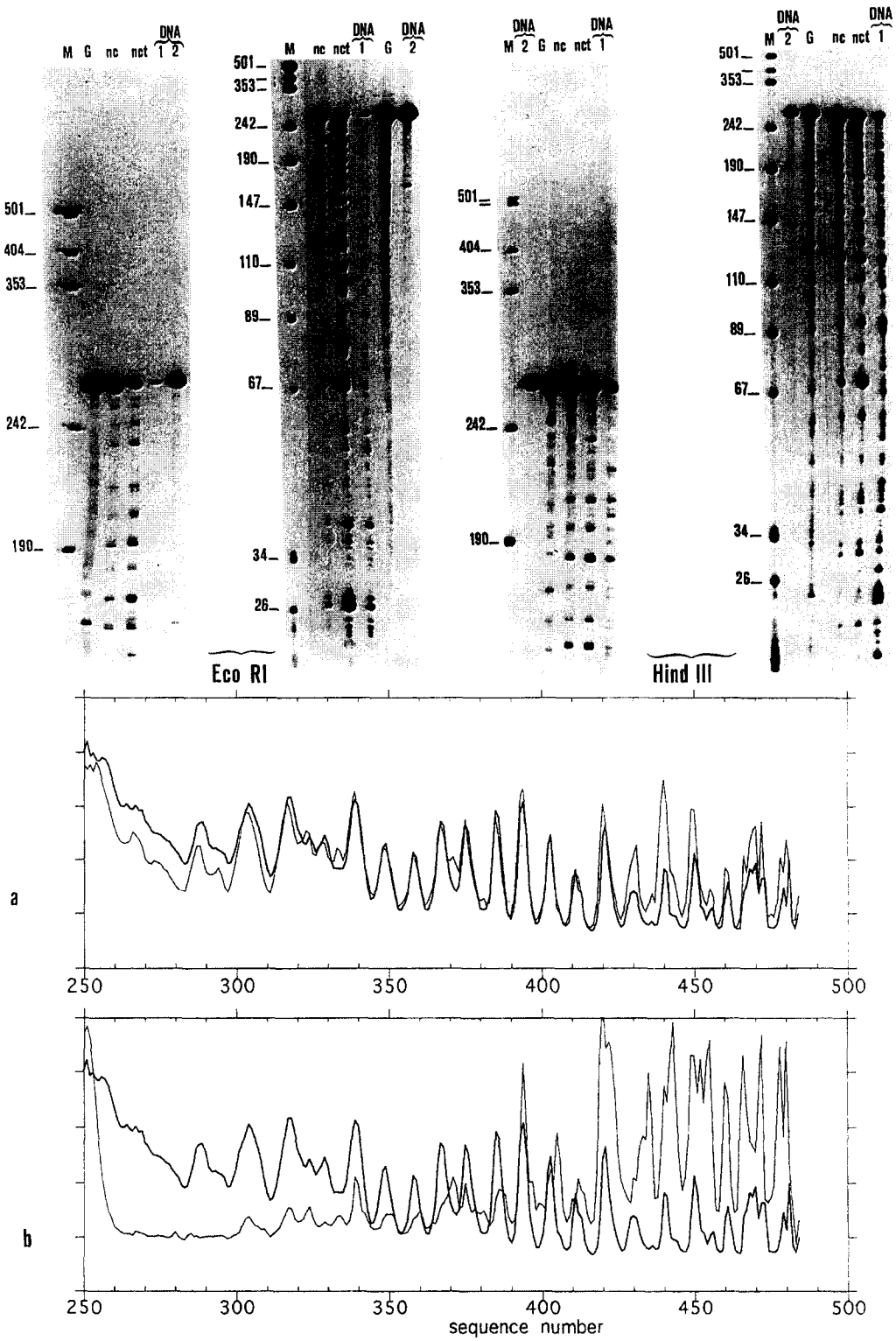
M G nc nct DNA 1 2
501
404
353
242
190
M nc nct DNA 1 G DNA 2
501
353
242
190
147
110
89
67
34
26
Eco RI
DNA M 2 G nc nct DNA 1
501
404
353
242
190
M DNA 2 G nc nct DNA 1
501
353
242
190
147
110
89
67
34
26
Hind III
a
250
300
350
400
450
500
b
250
300
350
400
450
500
sequence number

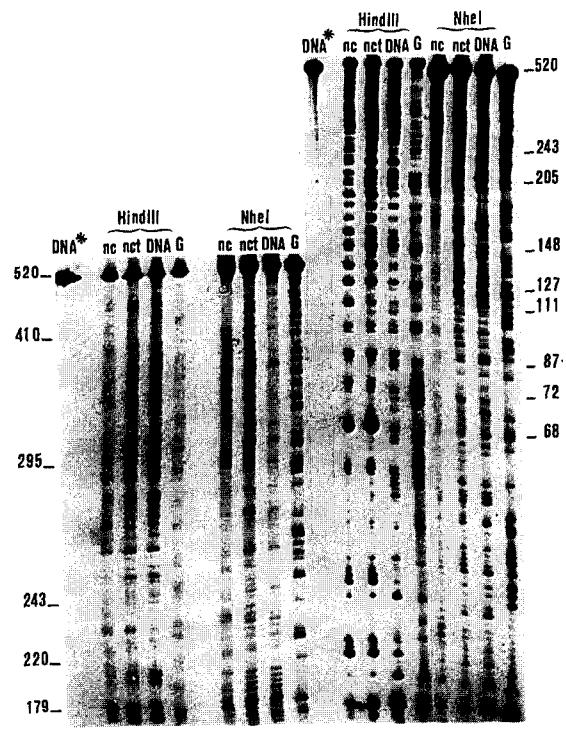
HindIII
NheI
DNA*
nc nct DNA G
520
410
295
243
220
179
520
243
205
148
127
111
87
72
68

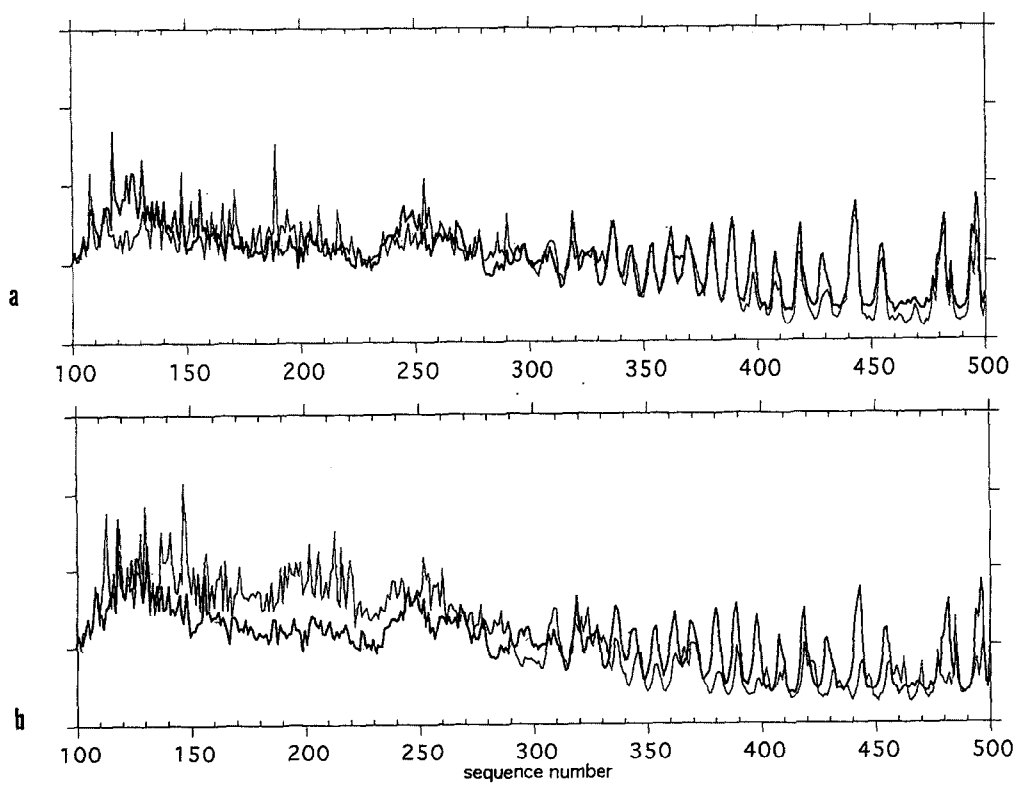
a
b
100 150 200 250 300 350 400 450 500
sequence number

that, whilst the trypsinized nucleosome appears to populate preferentially the region adjacent to the first nucleosome on the *C. fasciculata* curved sequence, centred at about 240 bp, the normal nucleosome appears to prefer the CT1 *Nhe* I extremity, since it is centred at about 100 bp.

3.4. DNAse I digestion analysis shows different superstructural features and nucleosome positioning in the two halves of the 520 bp DNA fragment

In order to obtain further evidence on the positioning of normal and 'tailless' histone octamer on CT1 and CT2 DNA fragments, DNAse I protection studies have been carried out. The DNAse I cutting patterns of CT1 5′-labelled at the *Hin*d III or at the *Nhe* I extremity, or of CT2 5′-labelled at the *Hin*d III or at the *Eco* RI extremity, are shown in Fig. 7 (top) and in Fig. 8 (top). The band pattern of DNAse I cleavage of the CT2 naked fragment (see Fig. 7 top, lane 1) shows a periodicity, more evident after the interaction of CT2 with normal or selectively trypsinized octamer (see Fig. 7 top, lanes nc and nct respectively).

These features of DNAse I cleavage patterns result more evident in the densitometric analysis reported in the same figure (bottom), where are reported for comparison (a) nc and nct; (b) nc and naked DNA. The periodicity in the case of complexed DNA, assigned by Fourier analysis, is about 10–11 bp, equal in the case of nc or nct. In the case of naked DNA the periodicity of cleavage appears practically equal to that of nc or nct, except that some bands appear less regular, split in two or three minor bands. Similar results were obtained if the DNAse I cleavage pattern of the same fragment, 5″-labelled at the *Eco* RI extremity, was analysed by densitometry (data not shown).

The DNAse I cleavage patterns of CT1, shown in Fig. 8 (top), are complex and not easily interpretable. Looking at the densitometric tracings, see Fig. 8 (bottom), however, it is evident that the fragment can be considered made by two halves. The moiety, corresponding to the CT2 fragment, shows the same bands periodicity as in the case of the shorter fragment. On the contrary, the other moiety does not show any appreciable regularity, neither in nc or nct.

These results show that the two nucleosomes, owing to the different superstructural features of the two moieties of CT1, have a very different behaviour. The first is positioned on the *C. fasciculata* curved sequence with the same rotational phase and translational multiplicity as in CT2. The second one does not oscillate about a unique preferential position, but can adopt at least two sets of multiple translational positions with the same rotational phase. These two sets, owing to the lack of regularity of their bands, correspond to nucleosome positions out of phase.

4. Discussion

In this article, the study of the respective influence of histone aminoterminal domains and DNA superstructural features on nucleosome positioning, has been carried out by the comparison between normal and selectively trypsinized nucleosome positioning, as well as between experimental and theoretical nucleosome positioning. The results reported in Fig. 5 clearly demonstrate that the normal and the tailless histone octamer are both positioned on the strongly curved *C. fasciculata* sequence, adopting a unique rotational setting, dictated by the superstructural features of this sequence. These results are in agreement with the potentiality of this highly curved sequence to act as a 'nucleosome attractor' [21]. Further, they agree with the recognition, by the octamer lacking the NH_2 terminal domains, of the

Fig. 8. (top) Autoradiography of DNAse I digestion patterns of CT1 (5′-labelled at the *Nhe* I and *Hin*d III sites) complexed with normal (nc) or selectively trypsinized histone octamer (nct). DNA*) naked DNA; DNA) DNase I digested naked DNA; G) positions of guanine in the sequence. (bottom) Densitometric tracings of nc - bold faced - and nct (a), and of nc - bold faced - and naked DNA (b) (data derived from the CT1 5′-labelled *Hin*d III site DNase I experiment).

same nucleosome positioning signals as in the case of the intact octamer, as shown by Dong et al. [11] on the *Lythechinus variegatus* 5S rRNA gene sequence and by Hayes et al [12] on the *Xenopus borealis* somatic 5S rRNA gene.

However, it is interesting to note that, using a quantitative approach, if the heights of the different maxima, caused by the translational multiplicity of the nucleosome positioning, are considered, the two types of nucleosomes occupy with different frequencies the different positions. That suggests that local specific interactions between histone side chains and DNA bases could be involved, although this topic deserves further investigations.

This model is further supported by DNase I analysis. The densitometric profiles, reported in Fig. 7 (bottom), in the case of nc and nct, present the same number of equivalent maxima. The spacing between the maxima is about 10–11 bp, as derived from Fourier analysis. These findings confirm that, in the limit of experimental errors, the mononucleosome translational multiplicity, with the same rotational phase, is equal in the two cases.

The comparison between virtual nucleosome dyad axis positioning reported in Fig. 4 and the normal and selectively trypsinized nucleosome dyad axis positioning reported in Fig. 5 (bottom) demonstrates a very satisfactory agreement between theoretical and experimental nucleosome positioning. It is worth noting that the adopted system, namely the *Crithidia fasciculata* sequence, can be considered fairly selective, since it is possible to test an extensive multiple nucleosome positioning.

Further, an interesting result comes out from DNase I study of the naked CT2 fragment, that is, also in this case, the periodicity of the cleavage bands. As it is possible to observe in Fig. 7b (bottom), where the densitometric tracing of naked DNA digested by DNase I is reported. The periodicity, as derived from Fourier analysis is about 10–11 bp. This finding allows us to picture CT2 in solution as a circle, in agreement with the theoretical prediction reported in Fig. 3B (bottom) and with the electron microscopy visualization of the same fragment carried out by Griffith et al. [19].

In the case of dinucleosome positioning on the CT1 fragment, the study was more difficult, since the second nucleosome appears able to adopt at least two different sets of translational positions, with the same rotational phasing.

These two sets are out of phase between each other. In fact, the fragment moiety, not derived from *Crithidia*, is practically straight with two almost equivalent tracts of opposite curvature (see the top of Fig. 3(B), where the stereoview of CT1 is reported). The theoretical prediction of two sets of nucleosome positions (with the same rotational phase), out of phase between each other, allows to predict the features of Exo III as well as of DNase I mapping of the second nucleosome. It is worth noting that our model locating the first and most stable nucleosome on the *Crithidia* curved sequence is supported by the theoretical analysis, Exo III cleavage patterns (see Fig. 6(a) (top)), Exo III analysis of mononucleosome on CT1 (not reported), and DNase I analysis reported in Fig. 8 (a) and (b) (bottom).

Exo III analysis of the second nucleosome can be carried out taking into account that Exo III mapping is able to discriminate between molecules having the second nucleosome positioned at the Nhe I end (centred at about 100 bp), or in the central tract of CT1 (centred at about 240 bp). In fact, considering the dyad axis positions reported in Fig. 6 (bottom), the two sets of nucleosome positions appear evident both in the case of nc and nct.

As for DNase I analysis, the overlapping of two sets of bands, rising from the cleavage of out of phase nucleosomes, gives rise to an irregular band pattern as shown in Fig. 8 (bottom).

Whereas the positioning of the second nucleosome, in the case of nc and nct, appears almost equal, the population of molecules with the second nucleosome oscillating about the intermediate position between *Nhe* I and *Hind* III sites (centred at about 240 bp) results different in the two cases (see Fig. 6 bottom). Namely, this intermediate position, which is adjacent to the first nucleosome positioned on the *Crithidia* curved sequence, is definitely more populated in the case of nct. This finding is also supported by the fact that the position, at the *Nhe* I extremity, centred at about 100 bp, is more populated in the case of nc (see also Fig. 6 bottom). Although it is impossible, at the moment, to attribute a precise structural meaning to this feature of nc and nct positioning, it is tempting to suggest that it could derive from the different ability of nc and nct to fold

the linker DNA, previously shown by Garcia-Ramirez et al. [14] in their study on the role of histone 'tails' in the folding of oligonucleosomes.

If the NH_2 terminal domains are necessary to fold linker DNA, it derives that the second nucleosome prefers to place in a position, with respect to the first nucleosome, that requires a lower energy cost in the linker folding. In fact, assuming that the first nucleosome and the second one can be considered centred respectively at 380 bp (I) and at 240 bp and/or 100 bp (II), some considerations about the linker can be made. If the two nucleosomes were centred respectively at 380 bp and at 240 bp, the linker would be practically absent, whilst, as shown by Yao et al. [24], it must be assumed that the average linker length is of the order of one persistence length. This consideration seems to explain the higher frequency of the second nucleosome population at 100 bp in the case of nc. The opposite behaviour in the case of nct can be attributed to the fact that, in this case, the dinucleosome does not require a linker. This model is also supported by our previous results on nc and nct organization on supercoiled and relaxed pBR322 DNA [13].

From the reported results, dinucleosome emerges as the minimum size model system to investigate the role of aminoterminal domains in chromatin organization. On the contrary, mononucleosome, as can be derived from previous qualitative results (11,12) and from our more quantitative approach (this article), appears as an inadequate model system.

Finally, it is worth considering that, since our theoretical prediction derives from the nearest-neighbour approximation, the obtained results show that this simple model is reliable in predicting DNA physico-chemical properties, such as gel electrophoretic mobility [25], cyclization probabilities [26], as well as specific interactions with normal and trypsinized histone octamer (this article).

Acknowledgements

Thanks are due to Massimo Arceci for preparation of plasmid pPK201/CAT and to CNR, Comitato Biotecnologie e Biologia Molecolare, for partial financial support.

References

[1] R.T. Simpson, Progress in Nucl. Acid Res. and Mol. Biol., 40 (1991) 143–184.
[2] T.E. Shrader and D.M. Crothers, J. Mol. Biol., 216 (1990) 69–84.
[3] H.R. Drew and A.A. Travers, J. Mol. Biol., 186 (1985) 773–790.
[4] S.C. Satchwell, H.R. Drew and A.A. Travers, J. Mol. Biol., 191 (1986) 659–675.
[5] K.E. van Holde, Chromatin (Springer Series in Molecular Biology) Springer–Verlag, New York, 1988, pp.257–260.
[6] M.G. Turnell and A.A. Travers, Methods in Enzymology, 212 (1992) 387–400.
[7] P. De Santis, M. Fuà, A. Palleschi and M. Savino, Biophys. Chem., 46 (1993) 193–204.
[8] L. Bohm and C. Crane-Robinson, Bioscience Reports, 4 (1984) 365–386.
[9] B.M. Turner, Cell, 75 (1993) 5–8.
[10] J. Ausio, F. Dong and K.E. van Holde, J. Mol. Biol., 206 (1989) 451–463.
[11] F. Dong, J.C. Hansen and K.E. van Holde, Proc. Natl. Acad. Sci. USA, 87 (1990) 5724–5728.
[12] J.J. Hayes, D.J. Clark and A.P. Wolffe, Proc. Natl. Acad. Sci. USA, 88 (1991) 6829–6833.
[13] M. Buttinelli, L. Leoni, B. Sampaolese and M. Savino, Nucl. Acids. Res., 19 (1991) 4543–4549.
[14] M. Garcia-Ramirez, F. Dong and J. Ausio, J. Biol. Chem., 267 (1992) 19587–19595.
[15] P.A. Kitchin, V.A. Klein, K.A. Ryan, K.L. Gamm, C.A. Ranch, D.S. Kang, R.D. Wells and P.T. Englund, J. Biol. Chem., 261 (1986) 11302–11309.
[16] P. Forte, L. Leoni, B. Sampaolese and M. Savino, Nucl. Acids Res., 17 (1989) 8683–8694.
[17] N. Ramsay, J. Mol. Biol., 189 (1986) 179–188.
[18] M. Buttinelli, G. Camilloni, G. Costanzo, R. Negri, P. Venditti, S. Venditti and E. Di. Mauro Methods in Molecular Genetics Vol. 6B, (1995) 168–185.
[19] J. Griffith, M. Bleyman, C.A. Rauch, P.A. Kitchin and P.T. Englund, Cell, 46 (1986) 717–724.
[20] P. De Santis, A. Palleschi, M. Savino and A. Scipioni, Biophys. Chem., 32 (1988) 305–317.
[21] G. Costanzo, E. Di Mauro, G. Salina and R. Negri, J. Mol. Biol., 216 (1990) 363–374.
[22] D. Boffelli, P. De Santis, A. Palleschi and M. Savino, Biophys. Chem., 39 (1991) 127–136.
[23] S. Cacchione, M.A. Cerone, P. De Santis and M. Savino, Biophys. Chem., 53 (1995) 267–281.
[24] J. Yao, P.T. Lowary and J. Widom, Proc. Natl. Acad. Sci. USA, 87 (1990) 7603–7607.
[25] S. Cacchione, P. De Santis, D. Foti, A. Palleschi and M. Savino, Biochemistry, 28 (1989) 8706–8713.
[26] S. Cacchione, P. De Santis and M. Savino, FEBS Lett., 336 (1993) 293–298.